ARTICLE

Probe the Effects of Surface Adsorbates on ZnO Nanowire Conductivity using Dielectric Force Microscopy

Qi Chen[a,b], Wei Lu[b], Yu-kun Wu[c], Huai-yi Ding[c], Bing Wang[a], Liwei Chen[b*]

a. Hefei National Laboratory for Physical Sciences at the Microscale, University of Science and Technology of China, Hefei 230026, China
b. i-Lab, Suzhou Institute of Nano-Tech and Nano-Bionics, Chinese Academy of Sciences, Suzhou 215123, China
c. Department of Physics, University of Science and Technology of China, Hefei 230026, China

(Dated: Received on May 7, 2014; Accepted on May 15, 2014)

Characterization of electric properties of nanomaterials usually involves fabricating field effect transistors (FET) and deriving materials properties from device performances. However, the quality of electrode contacts in FET devices heavily influences the device performance, which makes it difficult to obtain the intrinsic electric properties of nanomaterials. Dielectric force microscopy (DFM), a contactless method developed recently, can detect the low-frequency dielectric responses of nanomaterials without electric contact, which avoids the influence of electric contact and can be used to study the intrinsic conductivity of nanomaterials. Here we study the influences of surface adsorbates on the conductivity of ZnO nanowires (NWs) by using FET and DFM methods. The conductivity of ZnO NW is much larger in N_2 atmosphere than that in ambient environment as measured by FET device, which is further proven by DFM measurement that the ZnO NW exhibits larger dielectric response in N_2 environment, and the influence of electrode contacts on measurement can be ruled out. Based on these results, it can be concluded that the adsorbates on ZnO NW surface highly influence the conductivity of ZnO NW rather than the electrode contact. This work also verifies the capability of DFM in measuring electric properties of nanomaterials.

Key words: Dielectric force microscopy, ZnO nanowire, Field-effect transistor, Surface adsorbate

I. INTRODUCTION

Nanomaterials [1–3], such as nanocrystals, nanowires, nanotubes and nanosheets, have been considered as fundamental building blocks for future nanoelectric devices because they exhibit superior electric properties than their bulk materials counterpart due to nano size effects.

ZnO nanowires (NWs) are one of the most widely investigated nanomaterials, which has great potential applications in ultraviolet photodetectors, light-emitting diodes, photovoltaic cells and piezoelectric devices [4–7]. But the electric properties of ZnO NW are sensitive to the adsorptive molecules on the surface, and the high surface-to-volume ratio further intensifies this influence [5, 8]. For practical applications of electric devices based on ZnO NWs, it is necessary to understand the influence of ambient environment, such as O_2 and H_2O molecules, on the electric properties of ZnO NWs [9, 10]. It has been reported that O_2 and H_2O molecules adsorbed on ZnO surface will capture mobile electrons in ZnO NW because of their high electric negativity, resulting in reduced carrier density and conductivity of ZnO NW [5, 8].

Usually, electric properties of NW materials were obtained by fabricating field effect transistor (FET) devices and measuring their transport properties [11, 12]. However, the FET measurements are highly dependent on the quality of devices, especially the metal contact between nanomaterials and external circuit. Electrode materials selection, delicate device fabrication, and even testing environment may significantly influence the results [13–15], making it difficult to unveil the intrinsic electric properties. In addition, FET device fabrication requires expensive nanofabrication facility and suffers from low throughput.

In order to solve these problems and probe the intrinsic electric properties of nanomaterials, a new technique named as dielectric force microscopy (DFM) was recently developed in our group [16–18]. DFM is a contactless method based on electric force microscopy (EFM) [19–27] to measure the low-frequency dielectric response of materials. It is known that the dielectric responses of metallic and semiconductor materials de-

*Author to whom correspondence should be addressed. E-mail: lwchen2008@sinano.ac.cn

 ©2014 Chinese Physical Society

pend on their carrier density (n) and mobility (μ), which reflects the conductivity (σ=$ne\mu$, where e is the elementary charge) of material. The advantage of DFM is its nondestructive characteristic with high throughput, and the high spatial resolution enables it to probe the electric properties of nanomaterials. Most importantly, it excludes the effects of electrode contacts and reveals the intrinsic transport properties of materials. By this technique, we have successfully identified the carrier type and conductivity in single walled carbon nanotubes (SWNTs) [16, 17].

In this work, we used both FET and DFM techniques to study the influences of surface adsorbates on the electric properties of ZnO NW. By comparing transport behaviors detected by FET device and the dielectric responses detected by DFM in ambient environment and pure N_2 atmosphere, we found that the conductivity of ZnO NW was higher in N_2 than ambient environment. The higher conductivity of ZnO NW measured by FET device in N_2 atmosphere originated from increased conductivity of ZnO NW rather than electrode contact barrier variation.

II. EXPERIMENTS

A. Sample preparation and FET device fabrication

The high-quality ZnO NWs were grown in a dual-temperature-zone horizontal tube furnace with the vapor phase transport and condensation (VPTC) method [28, 29]. The diameter of ZnO NWs ranges from 100 nm to 130 nm, and their lengths are about 15 μm. By using PDMS stamping method, ZnO NWs were transferred onto a Si(100) wafer (∼0.01 Ω·cm) with 50 nm thermal oxide layer for DFM measurement, and to a Si(100) wafer (∼0.7 Ω·cm) with 300 nm thermal oxide layer for FET device fabrication and analysis.

For ZnO NW FET devices, 20 nm Ti/200 nm Au were deposited as electrodes via e-beam evaporation, and the distance between source and drain was 5 μm. Then the devices were rapidly annealed at 300−400 °C to improve the quality of contacts between the electrode and the ZnO NW.

B. DFM imaging experiments

DFM imaging was carried out on a Park XE-120 atomic force microscope (AFM) (Park Systems Corp., Suwon, Korea) using conducting AFM tips (NSC19/Ti-Pt, Mikromasch, Tallinn, Estonia) with a resonance frequency of about 80 kHz and spring constant of about 0.6 N/m. DFM imaging uses a two-pass scan mode as illustrated in Fig.1, which was developed from EFM technique. In the first pass, the standard AC mode imaging was performed to get topography of sample and the scan line was linearly fitted to obtain baseline. In the second pass, the tip was lifted up to a certain height

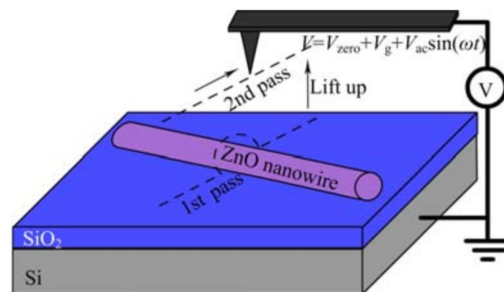

FIG. 1 Schematic illustration of dielectric force microscopy imaging operation mode.

and scanned in a trace parallel to the topographic baseline while turning off the cantilever oscillation at its resonance frequency. The key point for DFM is that a bias voltage was applied between substrate and tip in the second pass

$$V = V_{\text{zero}} + V_{\text{g}} + V_{\text{ac}} \sin(\omega t) \tag{1}$$

which was provided by a function generator (33522A, Agilent Technologies Inc., Santa Clara, CA, USA). Here, V_{zero} was adjustable DC voltage component to zero out the contact potential difference between the tip and the substrate [30–32], V_{g} was the DC voltage component that modulated the local carrier density in the NW, which varied between −4 and +4 V in the measurement; V_{ac}=6V_{peak} was the amplitude of an AC signal, and the frequency ω (typically 10 kHz) was set to be far below the cantilever resonance, thus only forced oscillation driven by electrostatic force was measured in the second pass. The $V_{\text{ac}} \sin(\omega t)$ between tip and substrate polarized the NW and resulted in an induced dipole moment osciallating in ω frequency. Since both the charges on the tip and the induced dipole on NW were proportional to $\sin(\omega t)$, the interaction force between NW and tip is proportional to

$$\sin^2(\omega t) = \frac{1}{2} - \frac{1}{2}\cos(2\omega t) \tag{2}$$

which contains attractive force oscillating in 2ω [16]. This force can be collected by a Stanford SR830 lock-in amplifier (Stanford Research System Inc., Sunnyvale, CA, USA) with 3 ms integration time. Then the measured dielectric response with 2ω was fed back to data acquasition software of AFM system to generate DFM images. In order to study the influence of adsorbate on ZnO NWs, the DFM measurement was conducted in a gas cell with ambient or N_2 atmosphere.

C. Device characterization and measurements

The morphology of ZnO NW FET devices were characterized by Hitachi S-4800 cold tip field emission scanning electron microscopy (Hitachi Hi-Tech Corp., Tokyo, JP). The current-voltage (I-V) characteristics of

DOI:10.1063/1674-0068/27/05/582-586
©2014 Chinese Physical Society

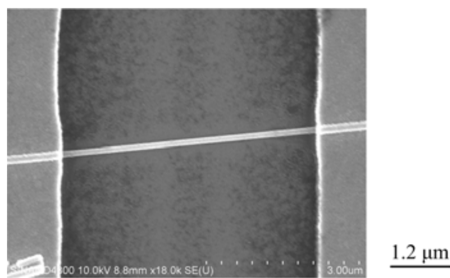

FIG. 2 SEM image of an individual ZnO nanowire field-effect transistor device.

the devices were measured using Agilent B1500A-SDA (Agilent Technologies Inc., Santa Clara, CA, USA) and Keithley 4200-SCS (Keithley Instruments Inc., Cleveland, OH, USA).

III. RESULTS AND DISCUSSION

Figure 2 is a SEM image of a ZnO NW FET device, the diameter of ZnO NW is 130 nm. The electric properties of the ZnO NW FET device in ambient and N_2 atmosphere are shown in Fig.3. The linear current (I_{sd}) versus voltage (V_{sd}) characteristics of the ZnO NW FET device with floating gate in Fig.3(a) clearly indicate a good Ohmic contact between electrodes and ZnO NW in both environments. And the ZnO NW exhibits much larger conductivity in N_2 atmosphere compared to that in ambient atmosphere. The transconductance curves in Fig.3(b) show similar on/off ratio around 1.7×10^5 in ambient and N_2 atmosphere, when gate voltage (V_g) sweeps from -20 V to $+30$ V. This means the ZnO NW exhibits a typical n-type semiconductor behavior both in N_2 and ambient atmosphere. However, threshold voltage (V_{th}) is shifted from -0.45 V in ambient to -2.37 V in N_2. V_{th} is the value of V_g when the conducting channel just begins to connect the source and drain contacts of the transistor, allowing significant current. Higher carriers density of device always has more negative V_{th}. In Fig.3(b), V_{th} in N_2 atmosphere shifted to more negative value, supportive the higher carrier density and higher conductivity [12]. Detailed parameters of ZnO NW FET device in ambient and N_2 atmosphere are listed in Table I, which shows little difference in mobility but larger carrier density and conductivity in N_2 atmosphere.

It is reported that adsorption of O_2 and/or H_2O molecules on the ZnO NW surface will capture mobile electrons and reduce the electron density. The possible reason for lower conductivity of ZnO NW FET device is the adsorbed molecules induced wider surface depletion region of ZnO NW [5], or increased contact barrier between electrode and ZnO NW [13, 33]. However, FET measurement itself is not enough to unravel the dominant factor because the measurement result is highly dependent on the quality of electrode contacts. Since

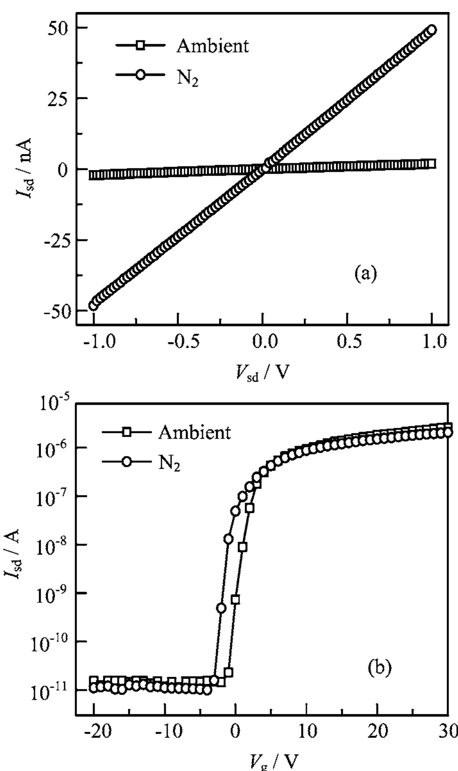

FIG. 3 Electric properties of the ZnO NWs characterized via FET transport measurements. (a) Current I_{sd} versus voltage V_{sd} characteristics of the ZnO NW FET device under floating gate in ambient and N_2 atmosphere. (b) Transconductance of the same device measured at a bias voltage (V_{sd}) of 1 V on a logarithmic scale in ambient and N_2 atmosphere with the gate voltage from -20 V to $+30$ V.

TABLE I Electric properties of ZnO NW FET device in ambient and N_2 atmosphere.

	Mobility/ $cm^2/(V{\cdot}s)$	Carrier/ cm^{-3}	Density/ S/cm	V_{th}/V
Ambient	29.94	1.55×10^{15}	7.41×10^{-3}	-0.45
N_2	23.82	4.78×10^{16}	0.182	-2.37

DFM can reflect the conductivity of materials without the interference of electrode contacts, we use this contactless technique to study the conductivity of individual ZnO NW without electrodes in ambient and N_2 environments.

Six ZnO NWs on one Si substrate were analyzized by DFM technique. Figure 4 (a)−(c) show increased dielectric responses of the ZnO NW under V_g of -4, 0, $+4$ V in ambient atmosphere, and DFM images of one ZnO NW with diameter of 130 nm are shown in Fig.4(d). After continuous N_2 flow (20 sccm) through the gas cell for 8 h to expel the O_2 and H_2O molecules adsorbed on ZnO NW, the ZnO NW was scanned by DFM again with the same setup [16]. Figure 4 (e)−(g)

DOI:10.1063/1674-0068/27/05/582-586 ©2014 Chinese Physical Society

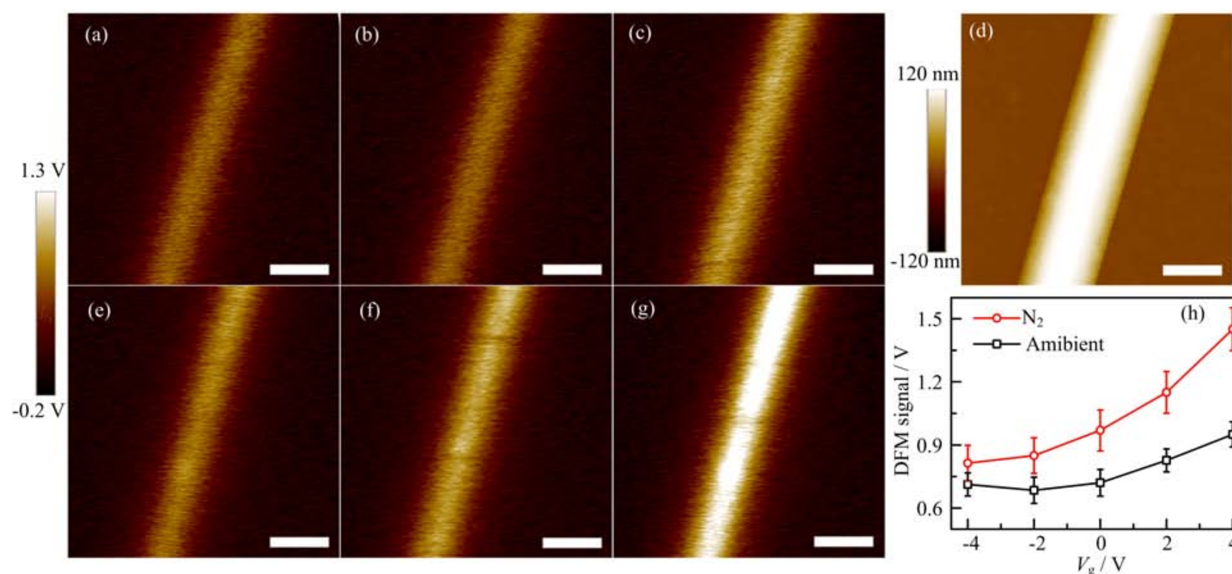

FIG. 4 (a)−(c) DFM images of a ZnO NW in ambient atmosphere at different value V_g of (a) −4 V, (b) 0 V and (c) +4 V. (d) Topography of ZnO NW with diameter of 130 nm. (e)−(f) DFM images of the same ZnO NW in N_2 atmosphere at V_g of (e) −4 V, (f) 0 V, and (g) +4 V. The scale bars are 200 nm. (h) DFM signal versus V_g plots for ZnO NW in ambient and N_2 atmosphere.

show the dielectric responses of ZnO NW under V_g of −4, 0, +4 V in N_2 environment. It is intriguing that ZnO NW in N_2 atmosphere not only increased dielectric response from V_g=−4 V to +4 V, but also enhanced dielectric responses compared to those in ambient atmosphere (Fig.4(h)).

In DFM measurement, the gate voltage between tip and substrate is similar to the gate voltage in FET device. When a negative gate voltage is applied to the tip, electrons are depleted in the region of NW just under the tip, and the concentration of charge carriers responding to AC electric field is reduced, which leads to a weaker dielectric response of ZnO NW. When a positive gate voltage is applied to the tip, electrons will accumulate under the tip, more charge carriers will response to the AC electric field induced by tip. The higher the positive gate voltage is applied, the more electrons will response to the AC electric field, which will increase dielectric response of ZnO NW. In ambient environment, O_2 and/or H_2O molecules adsorbed on ZnO NW surfaces will interact and capture mobile electrons, resulting in lower concentration of charge carriers than that in nitrogen atmosphere. Thus the dielectric response of ZnO NW is weaker in ambient environment than that in nitrogen atmosphere. Therefore, the trend of conductivity measured by ZnO NW FET device is consistent with dielectric responses measured by DFM.

It is worth noting that in ZnO FET device, the transport behaviors are influenced by the electric properties of ZnO NW and the electrode contacts simultaneously. On the contrary, ZnO NW investigated by DFM has no electrode contacts, whose variation of dielectric responses with different gate voltages comes from the charge carrier redistribution only [16]. Therefore, DFM results provide a direct evidence that the reducution of conductivity of ZnO NW FET device in ambient atmosphere was originated from decreased conductivity of ZnO NW rather than electrode contacts barrier variation.

The reasons that ZnO NW exhibits different conductivity in ambient and N_2 atmosphere can be rationalized in Fig.5. Generally, ZnO is a n-type semiconductor, because of its donor type defect states, such as oxygen vacancy and zinc interstitial [34]. In ambient atmosphere (Fig.5(a)), high surface-to-volume ratio of ZnO NW facilitates O_2 and/or H_2O adsorption, and the adsorbed molecules with high electric negativity will anchor mobile electrons, resulting in reduced concentration of free electrons and lowered Fermi level (E_F). A depletion region with lower conductivity is formed, thus the conductivity of ZnO NW is suppressed. When a continuous nitrogen gas flow is introduced to expel the O_2 and/or H_2O molecules from the surface of ZnO NW, the immobilized electrons are released, and the concentration of mobile electrons increases and Fermi level raises [35]. This process reduces the surface depletion region and recovers the conductivity of ZnO NW (Fig.5(b)). So, ZnO NW exhibits higher conductivity in N_2 atmosphere than that in ambient atmosphere.

IV. CONCLUSION

Both electric properties measured by FET device and dielectric response detected by DFM are carried out on individual ZnO NW in ambient and N_2 atmosphere. The DFM measurement confirms that lower conductiv-

DOI:10.1063/1674-0068/27/05/582-586 ©2014 Chinese Physical Society

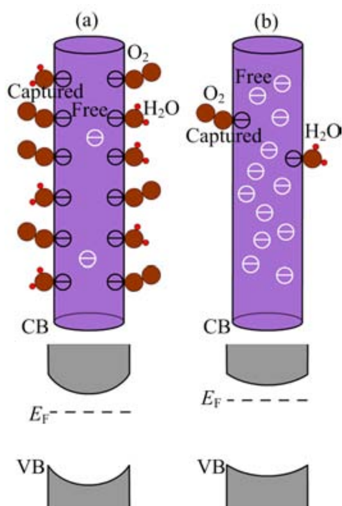

FIG. 5 Schematics and energy band diagrams of ZnO NW in (a) ambient and (b) N_2 atmosphere.

ity of ZnO NW measured by FET device in ambient environment than that in N_2 atmosphere is originated from reduced intrinsic conductivity of ZnO NW due to surface adsorbates, rather than increased electrode contacts barrier. The mechanism is rationalized by energy band diagram. Our result further supports that DFM is a powerful tool in probing intrinsic transport properties of nanomaterials.

V. ACKNOWLEDGMENTS

The authors appreciate the Nanofabrication Facility and the Electron Microscope Lab at SINANO, CAS for their help in device fabrication. This work was supported by the National Natural Science Foundation of China (No.11034001 and No.10904105).

[1] Y. Li, F. Qian, J. Xiang, and C. M. Lieber, Mater. Today **9**, 18 (2006).
[2] J. T. Hu, T. W. Odom, and C. M. Lieber, Accounts. Chem. Res. **32**, 435 (1999).
[3] C. Dekker, Phys. Today **52**, 22 (1999).
[4] Z. L. Wang and J. H. Song, Science **312**, 242 (2006).
[5] C. Soci, A. Zhang, B. Xiang, S. A. Dayeh, D. P. R. Aplin, J. Park, X. Y. Bao, Y. H. Lo, and D. Wang, Nano Lett. **7**, 1003 (2007).
[6] M. Law, L. E. Greene, J. C. Johnson, R. Saykally, and P. Yang, Nat. Mater. **4**, 455 (2005).
[7] X. W. Sun, J. Z. Huang, J. X. Wang, and Z. Xu, Nano Lett. **8**, 1219 (2008).
[8] H. Kind, H. Q. Yan, B. Messer, M. Law, and P. D. Yang, Adv. Mater. **14**, 158 (2002).
[9] R. D. Sun, A. Nakajima, A. Fujishima, T. Watanabe, and K. Hashimoto, J. Phys. Chem. B **105**, 1984 (2001).
[10] S. E. Ahn, J. S. Lee, H. Kim, S. Kim, B. H. Kang, K. H. Kim, and G. T. Kim, Appl. Phys. Lett. **84**, 5022 (2004).
[11] Y. Cui, X. F. Duan, J. T. Hu, and C. M. Lieber, J. Phys. Chem. B **104**, 5213 (2000).
[12] R. Martel, T. Schmidt, H. R. Shea, T. Hertel, and P. Avouris, Appl. Phys. Lett. **73**, 2447 (1998).
[13] Z. H. Chen, J. Appenzeller, J. Knoch, Y. M. Lin, and P. Avouris, Nano Lett. **5**, 1497 (2005).
[14] D. Mann, A. Javey, J. Kong, Q. Wang, and H. J. Dai, Nano Lett. **3**, 1541 (2003).
[15] S. B. Liang, Z. Y. Zhang, T. Pei, R. M. Li, Y. Li, and L. M. Peng, Nano Res. **6**, 535 (2013).
[16] W. Lu, J. Zhang, Y. S. Li, Q. Chen, X. P. Wang, A. Hassanien, and L. W. Chen, J. Phys. Chem. C **116**, 7158 (2012).
[17] J. Zhang, W. Lu, Y. S. Li, D. Lu, T. Zhang, X. Wang, and L. Chen, J. Phys. Chem. Lett. **3**, 3509 (2012).
[18] Y. S. Li, J. Ge, J. H. Cai, J. Zhang, W. Lu, J. Liu, and L. W. Chen, Nano Res. DOI 10.1007/s12274-014-0522-z
[19] O. Cherniavskaya, L. W. Chen, V. Weng, L. Yuditsky, and L. E. Brus, J. Phys. Chem. B **107**, 1525 (2003).
[20] W. Lu, D. Wang, and L. W. Chen, Nano Lett. **7**, 2729 (2007).
[21] W. Lu, Y. Xiong, A. Hassanien, W. Zhao, M. Zheng, and L. W. Chen, Nano Lett. **9**, 1668 (2009).
[22] R. Wang, S. N. Wang, D. D. Zhang, Z. J. Li, Y. Fang, and X. H. Qiu, ACS Nano **5**, 408 (2011).
[23] L. W. Chen, O. Cherniavskaya, A. Shalek, and L. E. Brus, Nano Lett. **5**, 2241 (2005).
[24] D. C. Coffey and D. S. Ginger, Nat. Mater. **5**, 735 (2006).
[25] A. Bachtold, M. S. Fuhrer, S. Plyasunov, M. Forero, E. H. Anderson, A. Zettl, and P. L. McEuen, Phys. Rev. Lett. **84**, 6082 (2000).
[26] L. W. Chen, R. Ludeke, X. D. Cui, A. G. Schrott, C. R. Kagan, and L. E. Brus, J. Phys. Chem. B **109**, 1834 (2005).
[27] W. Lu, Y. Xiong, and L. Chen, J. Phys. Chem. C **113**, 10337 (2009).
[28] H. Y. Ding, Z. Zhao, G. H. Zhang, Y. K. Wu, Z. W. Gao, J. W. Li, K. Zhang, N. Pan, and X. P. Wang, J. Phys. Chem. C **116**, 17294 (2012).
[29] Q. Chen, H. Ding, Y. Wu, M. Sui, W. Lu, B. Wang, W. Su, Z. Cui, and L. Chen, Nanoscale **5**, 4162 (2013).
[30] H. Ishii, N. Hayashi, E. Ito, Y. Washizu, K. Sugi, Y. Kimura, M. Niwano, Y. Ouchi, and K. Seki, Phys. Status. Solidi. A **201**, 1075 (2004).
[31] L. S. C. Pingree, O. G. Reid, and D. S. Ginger, Adv. Mater. **21**, 19 (2009).
[32] F. Chen, Q. Chen, L. Mao, Y. Wang, X. Huang, W. Lu, B. Wang, and L. Chen, Nanotechnology **24**, 484011 (2013).
[33] J. Zhou, Y. Gu, Y. Hu, W. Mai, P. H. Yeh, G. Bao, A. K. Sood, D. L. Polla, and Z. L. Wang, Appl. Phys. Lett. **94**, 191103 (2009).
[34] U. Ozgur, Y. I. Alivov, C. Liu, A. Teke, M. A. Reshchikov, S. Dogan, V. Avrutin, S. J. Cho, and H. Morkoc, J. Appl. Phys. **98**, 041301 (2005).
[35] S. Hullavarad, N. Hullavarad, D. Look, and B. Claflin, Nanoscale Res. Lett. **4**, 1421 (2009).

DOI:10.1063/1674-0068/27/05/582-586 ©2014 Chinese Physical Society